The Fourth International Conference on Mechanics and Energy
ICME'2018, December 20-22, 2018, Hammamet, TUNISIA
Web site: http://www.icme.aicme.net

CERTIFICATION OF PAPER PRESENTATION

This is to certify that Mr./Ms **Badis BAKRI** has participated in the Fourth International Conference on Mechanics and Energy (ICME'2018) with a **Poster** entitled:

Study of the Natural Convection Flow in a Solar Air Heater Test Bench

Author(s): *Badis BAKRI, Hani BENGUESMIA, Zied DRISS, Ahmed KETATA, Slah DRISS, Oumaima ELEUCH*

ICME 2018 Chair
Professor Mohamed Salah ABID

Study of the Natural Convection Flow in a Solar Air Heater Test Bench

Badis Bakri[1,2,*], Hani Benguesmia[2], Zied Driss[1], Ahmed Ketata[1], Slah Driss[1], Oumaima Eleuch[1]

Laboratory of Electro-Mechanic Systems (LASEM), NationalSchool of Engineers of Sfax (ENIS), University of Sfax (US), B.P. 1173, Road Soukra km 3.5, 3038 Sfax, TUNISIA

[2]Faculty of Technologies, University of M'sila, ALGERIA

Abstract: Improving air quality can support efforts to mitigate climate change. The challenge that we are facing is, therefore, to ensure that our air and climate policies focus on win-win scenarios. For this, we have studied the heat convection flow in a new solar air heater test bench, available in our LASEM laboratory. By using the ANSYS Fluent 17.0 software, the analysis was performed using the Navier-Stokes equations coupled with the standard k-ω turbulence model. The computational method and the simulation results were validated based on our experimental results developed in a tow passage solar air heater connected to a box prototype. The range of temperatures is very useful in many applications such as industrial and domestic applications.

Keys words: Solar air heaters, test bench, tow passages, box prototype, aerodynamic structure.

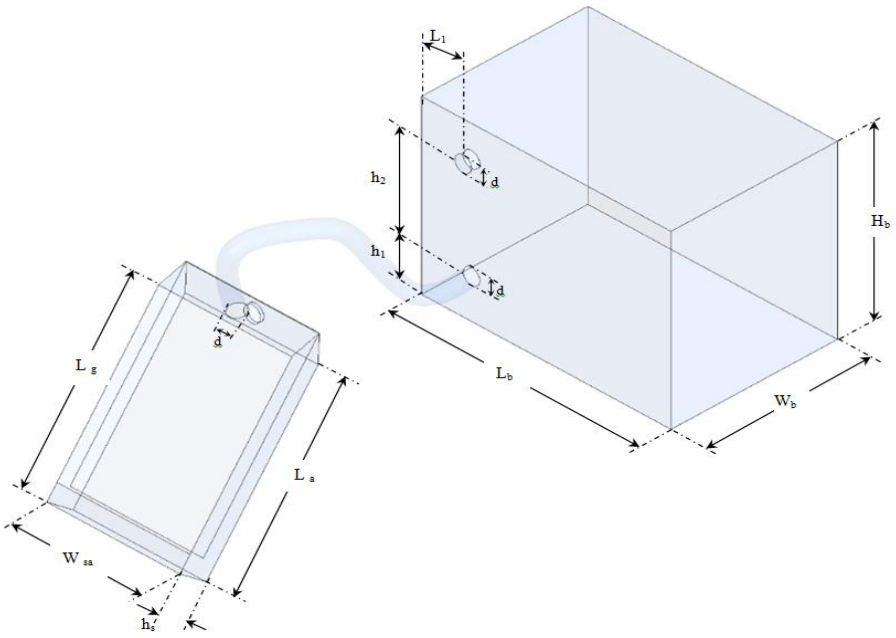

Graphical abstract

***Correspondingauthor:** Badis Bakri
E-mail: badisbakri@yahoo.fr.

1. Introduction

The natural convection flow in the solar air heater is widely considered by the designers and it was the subject of many researches [1-3]. For example, Nithiarasu et al. [4] studied the natural convection flow in a combined enclosure. Morsi and Das [5] analyzed the heat transfer and free convective motion for various structures. The numerical calculation of the flow in an enclosure with different dome configurations was developed based on a finite element method. Bocu and Altac [6] developed a numerical study of the natural convection flow in rectangular enclosures with pins. El-Sebaiietal. [7] compared the temperatures of the outlet air and the absorber plate for the double pass-finned solar air heater design with the corrugated plate. The results confirmed that the second design is more efficient compared to the first. Wazed et al. [8] compared the forced and natural circulation of the air flow in a solar air heater working efficiently. Sopian et al. [9] confirmed that the porous media addition increases the performance of the double-pass solar collector. The experimental validation revealed that the theoretical simulation were in close agreement with the experimental data. Esen et al. [10] developed an experimental study for a novel solar air heater with and without obstacles. The maximum value of efficiency is obtained for the double-flow collector provided with obstacles. Ozgen et al. [11] investigated a device for using an absorbing plate with aluminum cans for the considered solar air heater. The highest efficiency had been obtained for a mass flow rate equal to 0.05 kg/s. Theodosius et al. [12] presented experimental-numerical comparison to give the precision of the CFD model. Du et al. [13] conducted experimental results measurements to present the characteristics of a Chinese house. Homodet al. [14] studied and proposed a new system by coupling reasons of internal conditions that are influenced by the outdoor environment. Terrados and Moreno [15] integrated the architectural concepts with energy efficient. Focusing on these anterior studies, it has been noted that the most published works were interested on the developing of the solar system to improve the heat ventilation and to minimise the energy consumption. For this purpose, we have developed numerical and experimental investigation of the natural convection flow in a new solar air heater test bench with two passages. The experimental validation of our numerical simulation is in close agreement with our experimental data.

2. Geometrical system

A new solar air heater test bench was designed and realized in our LASEM laboratory to investigate the efficiency of the solar system. The considered system consists of a tow passages solar air heater separated by an absorber and powered by a fan working in a delivery mode and placed in the inlet, side the insulation. On the glass side, it is connected to the box prototype through a pipe. The geometrical arrangements of the computational domain are presented in figure 1, which is composed of two domains separated by a circular pipe with a diameter d=100 mm. The first one is the solar air heater with a height hs=194 mm and a width Ws=778 mm. On this system, a glass is hanging on the front side with a length Lg=1000 mm and an absorber is inserted inside with a length La=1086 mm. The hot air flow is routed towards the box prototype with a length Lb=1500 mm, a height Hb=1100 mm and a width Wb=1000 mm. Two circular holes, with a distance h2=900 mm, are located in the same face of the box prototype. The inlet holes, placed in the altitude h1=250 mm and a longitude L1=300 mm, allows the hot air supply. However, the outlet holes allow its escape into the ambient environment.

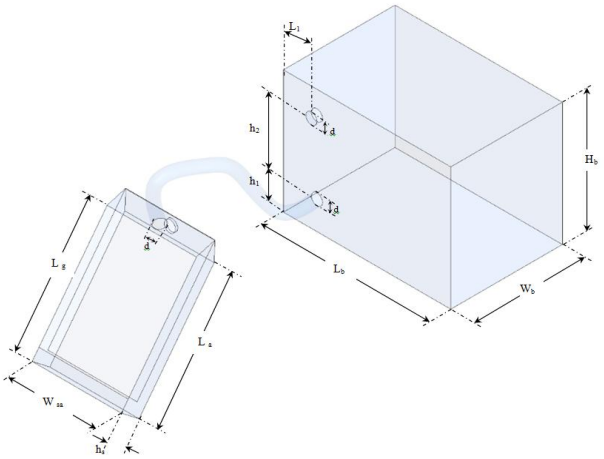

Fig. 1 Geometrical arrangement

3. Numerical model

The boundary conditions of the solar air heater test bench are illustrated in figure 2. Wall boundary condition was applied for the solar air heater with a heat flux of value equal to zero, corresponding to the adiabatic wall. Wall boundary was used for the absorber and the glass. Convective heat transfer option was applied for different parts of the device such as glass and absorber. For the pressure inlet and the pressure outlet, a value of p=101325 Pa was set. This means that at these openings, the fluid enters from the holes inlet and exits the model through the holes outlet.

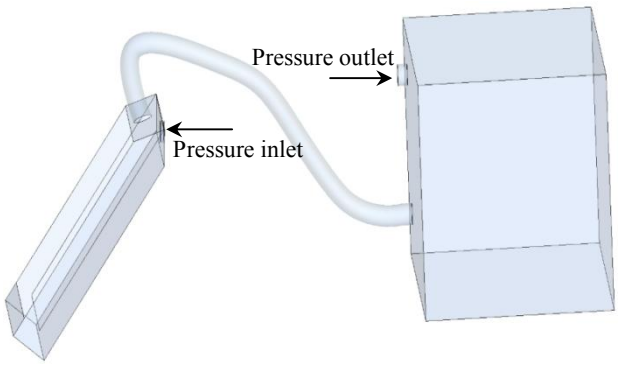

Fig. 2 Boundary conditions

The generated meshing is developed using the package ANSYS ICEM CFD. In this application, we have adopted the refined model consisting of a maximum number of cells equal to N=1578369 cells that gives the lower numerical diffusion inside the solar air heater with an unstructured and tetrahedral meshing as presented in figure 3.

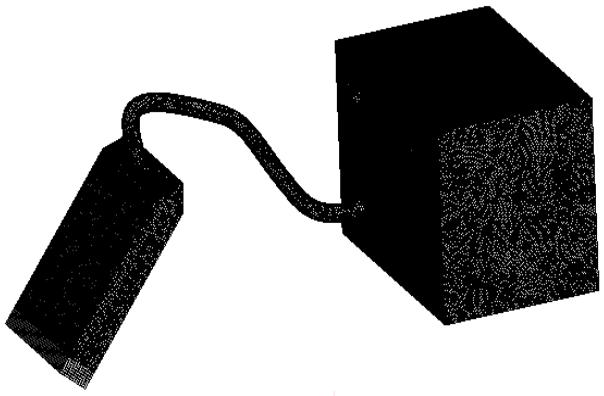

Fig. 3 Meshing of the computational domain

4. Results and discussion

The distribution of the velocity fields, the temperature, the total pressure and the turbulent viscosity are presented in this section. In the present work, the Reynolds number is evaluated and it is equal to Re=5100.

4.1 Velocity fields

Figure 4 shows the velocity fields distribution in the different longitudinal and transverse planes for the first and second passage of the solar air heater supplying the box prototype. According to these results, it is clear that the velocity inlet presents a weak value equal to V=0.2 $m.s^{-1}$. At the first passage, an increase of the flow has been observed in the first passage of the solar air heater. The maximum value equal to V=0.5 $m.s^{-1}$ has been noted at the beginning of the flow. From the middle of the first passage of the solar air heater, the velocity drops slowly until the solar air heater bottom. At this level, the velocity

value is equal to V=0.15 $m.s^{-1}$. Indeed, different recirculation zones are observed along the second passage of the solar air heater. At this level, the velocity value is very weak and it is about V=0.5 $m.s^{-1}$. Crossing the pipe separating the solar air heater from the box prototype, the velocity reaches V=0.25 $m.s^{-1}$. Via the box prototype holes inlet, a discharge area invaded the reverse wall. In this side, the velocity changes his direction and two axial flows have been observed. The first ascending flow is responsible for the recirculation zone appeared in the whole area of the box prototype. This movement continues until the exit of the air flow through the holes outlet and reaches the maximum value equal to V=0.23 $m.s^{-1}$. The second descending flow is due to the dead zone appeared in the down area. Globally, the averaged velocity value is about V=0.1 $m.s^{-1}$ in the discharge area.

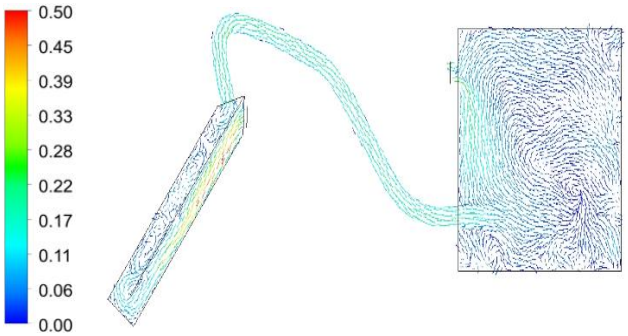

Fig. 4 Distribution of the velocity field

4.2 Total temperature

Figure 4 shows the temperature distribution in the different longitudinal and transverse planes for the first and second passages of the solar air heater supplying the box prototype. From these results, it has been noted that the inlet temperature is governed by the boundary conditions defined by T=308 K. This value increases immensely and reaches an average value equal to T=339 K in the first passage and T=345 K in the second passage. This fact can be explained by the air flow incoming at ambient temperature and flowing the channel between the absorber plate and the insulation, which start swarming up by the convection with the absorber. In the second passage, the temperature of the air flow is more important since the flowing between the glass and the absorber is affected by the solar radiations. Thereby, the box prototype is powered by a continuous air heater characterized by the maximum temperature value equal to T=349 K. In the holes outlet of the box prototype, the temperature drops and reaches T=308 K.

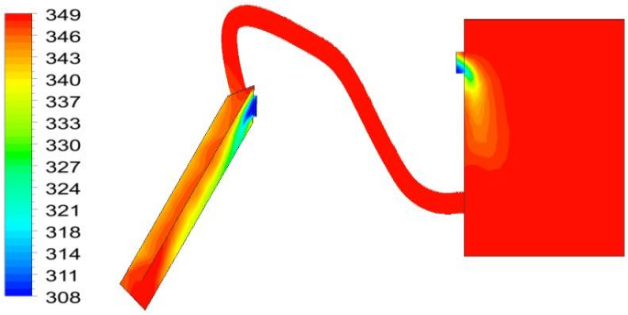

Fig. 5 Distribution of the total temperature

4.3 Total pressure

Figure 5 shows the total pressure distribution in the different longitudinal and transverse planes for the first and second passages of the solar air heater supplying the box prototype. According to these results, it is clear that the pressure inlet is governed by the boundary condition defined by the atmospheric pressure p=101325 Pa. Then, the total pressure decreases weakly at the bottom of the solar air heater and reaches p=101324 Pa. From this side, the total pressure increases slightly in the second passage of the solar air heater. At the exit of the second passage, the total pressure continues increasing along the pipe and reaches a value equal to p=101326 Pa at the first half part of the pipe separating the solar air heater from the box prototype. From the holes inlet of the box prototype roof, there is a slight increase of the total pressure until the box prototype roof. In this side, the

maximum value of the total pressure is equal to p=101326 Pa. In the holes outlet of the box prototype, it is governed by the boundary condition defined by the atmospheric pressure p=101325 Pa.

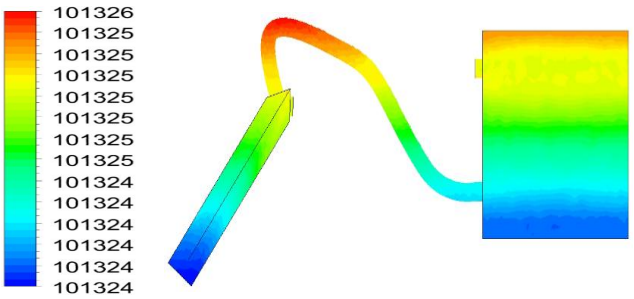

Fig. 6 Distribution of the total pressure

4.4 Turbulent viscosity

Figure 7 shows the turbulent viscosity distribution in the different longitudinal and transverse planes for the first and second passages of the solar air heater supplying the box prototype. According to these results, a weak value of the turbulent viscosity has been observed at the collector inlet of the solar air heater. Behind this area, a wake zone characteristic of the maximum value of the turbulent viscosity has been observed and expanded in the first passage near the absorber side. In these conditions, the maximum value of the turbulent viscosity is equal to μ_t=0.022 kg.m^{-1}.s^{-1}. Away from this area, the turbulent viscosity presents a very weak value. The same fact has been observed in the second passage, where the maximum value is equal to μ_t=0.009 kg.m^{-1}.s^{-1} in the first mid-plane. In the absorber, the turbulent viscosity reaches a weak value. At the exit of the second passage, a slight increase of the turbulent viscosity until μ_t=0.029 kg.m^{-1}.s^{-1} has been observed in the first part of the pipe connecting the solar air heater with the box prototype. In the remainder of the pipe, the turbulent viscosity decreases and presents very low values. In the holes inlet of the box prototype, the low values of the turbulent viscosity continue to appear in the first part of the discharge area. In the second part, a slight increase of the turbulent viscosity has been noted on the side of the reverse wall. In the rest of the domain of the box prototype, a weak value of the turbulent viscosity has been observed. This fact can be explained by the recirculation zone appeared in the whole area of the box prototype. Indeed, a slight expansion of the turbulent viscosity until μ_t=0.011 kg.m^{-1}.s^{-1} has been observed in the box prototype upper and the holes outlet.

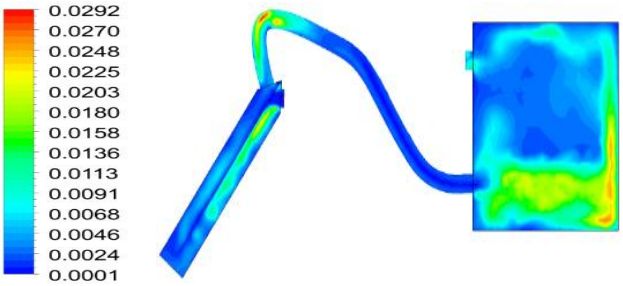

Fig. 7 Distribution of the turbulent viscosity

5. Comparison with experimental results

Figure 8 compare the numerical results of the velocity profiles in the second channel superposed with our experimental results in natural convection. According to these results, a similar appearance between the curves of the experimental and numerical results has been observed. The gap between the curves is about 6%. The good agreement confirms the validity of the numerical method.

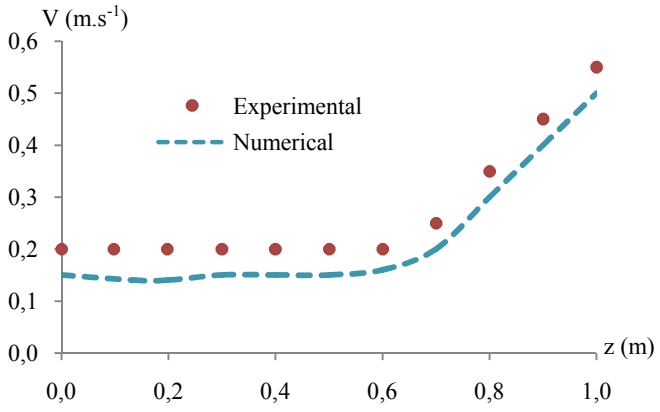

Fig. 8 Velocity profile in the second channel

6. Conclusion

The solar air heater is an interesting technology that is not very commonly used in the domestic and industrial applications. For this, we are interested in the design and the realization of a new solar air heater test bench to investigate the efficiency of the solar system. The considered system consists of a tow passages solar air heater separated by an absorber with natural convection, side the insulation. On the glass side, it is connected to the box prototype through a pipe. On this system, a glass is hanging on the front side and an absorber is inserted inside. The hot air flow is routed towards the box prototype. Two circular holes are located on the same face of the box prototype. The inlet holes allow the hot air supply. However, the outlet holes allow its escape into the ambient environment. Indeed, we have developed numerical simulations to study the natural convection flow in the considered test bench. In these conditions, the maximum value of the velocity has been noted at the beginning of the flow. From the middle of the first passage of the solar air heater, the velocity drops slowly until the bottom of the solar air heater. Along the second passage of the solar air heater, different recirculation zones have been observed. Via the box prototype holes inlet, a discharge area invaded the reverse wall. In this side, the velocity changes his direction and two axial flows have been observed. The first ascending flow is responsible for the recirculation zone appeared in the wholes area of the box prototype. Also, it has been noted that the inlet temperature is governed by the boundary condition. This fact can be explained by the air flow incoming at ambient temperature and flowing the channel between the absorber plate and the insulation, which start swarming up by the convection with the absorber. In the second passage, the temperature of the air flow is more important since the flowing between the glass and the absorber is affected by the solar radiations.

Thereby, the box prototype is powered by a continuous air heater characterized by the maximum value. This technology will be very useful since it can provide sustainable energy and substitute the expensive traditional technologies.

Nomenclature

Symbols :

T	temperature, K
k	turbulent kinetic energy, $m^2.s^{-2}$
p	total pressure, Pa
Re	Reynolds number, dimensionless
V	magnitude velocity, $m.s^{-1}$
x	first cartesian coordinate, m
y	second cartesian coordinate, m
z	third cartesian coordinate, m

Greek Letters:

ω	turbulent kinetic energy dissipation, s^{-1}
μ_t	turbulent viscosity, $kg.m^{-1}.s^{-1}$

Acknowledgments

The authors would like to thank the Laboratory of Electro Mechanic Systems (LASEM) members for the financial assistance.

References

[1] El-Gendi, "Transient turbulent simulation of natural convection flows induced by a room heater", International Journal of Thermal Sciences 125 (2018) 369–380.

[2] G. De Vahl Davis, "Natural convection of air in a square cavity: a bench mark numerical solution", Int J Numer Meth Fluid 3 (1983) 249–264.

[3] G. Barakos, E. Mitsoulis, D. Assimacopoulos, "Natural convection flow in a square cavity revisited: laminar and turbulent models with wall functions", Int J Numer Meth Fluid 18 (1994) 695–719.

[4] P. Nithiarasu, T. Sundararajan, K. N. Seetharamu, Finite element analysis of transient natural convection in an odd-shaped enclosure, Int J Numer Meth Heat Fluid Flow 8 (1998) 199–216.

[5] Y. S. Morsi, S. Das, Numerical investigation of natural convection inside complex enclosures, Heat Tran Eng 24 (2003) 30–41.

[6] Z. Bocu, Z. Altac, Laminar natural convection heat transfer and air flow in three dimensional rectangular enclosures with pin arrays attached to hot wall, Appl Therm Eng 31 (2011) 3189–3195.

[7] A. A. El-Sebaii, S. Aboul-Enein, M. R. I. Ramadan, S. M. Shalaby, B. M. Moharram, Thermal performance investigation of double pass-finned plate solar airheater, Applied Energy, 88 (2011) 1727–1739.

[8] M. A. Wazed, Y. Nukman, M. T. Islam, Design fabrication of a cost effective solar air heater for Bangladesh, Applied Energy, 87 (2010) 3030–3036.

[9] K. Sopian, M. A. Alghoul, M. A. Ebrahim, M. Y. Sulaiman, E. A. Musa, Evaluation of thermal efficiency of double-pass solar collector with porous-nonporousmedia, Renewable Energy, 34 (2009) 640-645.

[10] H. Esen, Experimental energy and exergy analysis of a double-flow solar airheater having different obstacles on absorber plates, Building and Environment, 43 (2008) 1046-1054.

[11] F. Ozgen, M. Esen, H. Esen, Experimental investigation of thermal performanceof a double-flow solar air heater having aluminum cans, Renewable Energy, 34 (2009) 2391-2398.

[12] C. Teodosiu, F. Kuznik, R. Teodosiu, CFD modeling of buoyancy driven cavities with internal heat source: Application to heated rooms, Energyand Buildings, 68 (2014) 403-411.

[13] X. Du, R. Bokel, A. V. D. Dobbelsteen, Building microclimate and summer thermal comfort in free-running buildings with diverse spaces: a Chinese vernacular house case, Building and Environment, 82 (2014) 215-227.

[14] R. Z. Homod, Assessment regarding energy saving and decoupling for different AHU (air handling unit) and control strategies in the hot-humid climatic region of Iraq, Energy, 74 (2014) 762-774.

[15] F. J. Terrados, D. Moreno, "Patio" and "Botijo": Energetic strategies' architectural integration in "Patio 2.12" prototype, Energy and Buildings, 83 (2014) 70–88.